Supporting Information

Defect engineering improves CO_2/N_2 and CH_4/N_2 separation performance of MOF-801

Chen-Ning Li [a], Wei-Guo Xu [a], Lin Liu [a,*], Zheng-Bo Han [a,*]

[a]*College of Chemistry, Liaoning University. Shenyang 110036, P. R. China*

*L. L.: E-mail: liulin@lnu.edu.cn

*Z.-B. H.: E-mail: ceshzb@lnu.edu.cn

1 Test method and calculation details

1.1 Gas adsorption isotherms test method

Before gas isothermal adsorption, new powder and methanol were switched out every 12 hours for three days to achieve thorough solvent exchange. Then it was heated to 393 K under vacuum for 12 hours, and N_2 isothermal adsorption was performed at 77 K using the 3H-2000PS2 instrument. The single-component gas adsorption capacities of CO_2, N_2 and CH_4 were then tested at 273K and 298K, in which a dewar was used to provide a constant temperature environment. The Brunauer-Emmett-Teller (BET) specific surface area and pore size distributions were calculated based on N_2 isothermal adsorption at 77 K, and the calculated results accord with the standard of the Rouquerol consistency criteria (with a linearity of fitting: $R > 0.9998$).[1–3]

1.2 Breakthrough experiments method

The breakthrough experiments were carried out in gas breakthrough equipment. The automatic equipment used in this study is designed by Nanjing Haoerpu Analytical Equipment Co., LTD. A 200 mm long tainless tube and 4 mm inner diameter was loaded with 1.4 g of MOFs (Figure S1). The sample column was first heated to 393 K under vacuum and fully activated overnight. The breakthrough experiments were conducted with a flow rate of 2 mL/min (50/50 v/v) CO_2/N_2 and (50/50 v/v) CH_4/N_2 binary mixture gas at 1 bar at room temperature, in order to obtain

the composition of the outlet gas more accurately, 2mL/min He was used as the tail dilution gas. All breakthrough tests were conducted under constant circumstances, and the constituents of the gases in the outflow were identified by online chromatography. The sample was reproduced with He flow (10 ml/min) at 353 K for 30 min after the breakthrough experiment for the next test.

1.3 Theoretical calculation method

In this study, the Single-site Langmuir-Freundlich (SLSF) model was used to correctly compute the IAST:[4,5]

$$N = A_1 \frac{b_1 P^{c_1}}{1+b_1 P^{c_1}} \qquad \text{Equation (S1)}$$

where N denotes gas uptake (mmol/g); A_1 represent the theoretical maximum adsorption capacity (mmol/g) at the 298 K; b_1 denote the correlation coefficients; c_1 denote the site anisotropism.

The IAST selectivity was calculated as follows:

$$S_{ij} = \frac{n_i/n_j}{y_i/y_j} \qquad \text{Equation (S2)}$$

In this scenario, i and j represent the two relative gases; n_i and n_j represent gas uptake; y_i and y_j represent the gas mixture's suggested mole fractions.

Based on the adsorption isotherms of pure gas at 298 K and 273 K, the isosteric enthalpies of adsorption were fitted to a virial equation[6] as follows:

$$lnP = lnN + \frac{1}{T}\sum_{i=0}^{m} a_i N^i + \sum_{i=0}^{n} b_i N^i \qquad \text{Equation (S3)}$$

where P denotes the pressure; N gives the amount of uptake; T refers to the temperature and m and n connote the number of words necessary to fully explain the

isotherm.

The fitting parameters were then used to calculate the isosteric heat of adsorption (Q_{st}) as follows:

$$Q_{st} = -R\sum_{i=0}^{m} a_i N^i \qquad \text{Equation (S4)}$$

Here R means the universal gas constant. The coverage dependence of the Q_{st} values was derived by fitting the adsorption data at various temperatures for MOFs.

2 Experimental sections

2.1 Materials and synthesis

Zirconium chloride ($ZrCl_4$, >98.0%) was offered from Shanghai Bidd Medical Technology Co., LTD. Fumaric acid (>99.0%) was purchased from China Pharmaceutical (Group) Shanghai Chemical Reagent, Formic acid (AR, >88%) was provided by Tianjin Damao Chemical Reagent Factory, and methanol (AR, >99.5%) was supplied from Tianjin Fuyu Fine Chemical Co., LTD. All reagents and solvents are used directly without further purification.

Zr-FA: The Dai et al.[7] technique is used to synthesize Zr-FA with a little modification. Initially, Zirconium chloride ($ZrCl_4$, 1.5 mmol, 350 mg) was placed in a round-bottomed flask with 2 mL formic acid and 8 mL deionized water, then stirred at room temperature for 20 min. Subsequently, fumaric acid (1.5 mmol, 175 mg) was then added to the solution. After overnight refluxing at 100 °C, a white solid was observed, indicating the formation of Zr-FA. The products were separated by

centrifugation, cleaned three times with ethanol and water, and then dried at 65 ºC using a continuous temperature drying oven, the yield was 89.2%.

Zr-FA_x: The synthesis methods of Zr-FA_x are similar to Zr-FA, except that the amount of formic acid is controlled to 4 mL (Zr-$FA_{0.5}$), 8 mL (Zr-FA_1), 16 mL (Zr-FA_2), and other synthesis conditions are the same.

2.2 Instrumentation

The Bruker AXS D8 system with Cu-K radiation (=1.5406) and a scanning range of 5 to 45° at a voltage of 40 kV and a current of 40 mA was used to acquire the powder X-ray diffraction (PXRD) pattern. Using a Nicolet 5DX at wavelengths between 4000 and 400 cm^{-1}, Fourier transform infrared spectroscopy (FT-IR) was utilized to identify the functional groups of the materials. The BeiShiDe 3H-2000PS2 system was used to demonstrate pore structure and surface characteristics of materials using N_2 adsorption-desorption isotherms at 77 K. Thermogravimetric analysis (TGA) was performed on a Precision RZY-1 thermogravimetric analyzer by increasing the temperature from ambient to 800 °C (10 °C/min in 10 mL/min nitrogen atmosphere).

3 Schematic diagram of breakthrough experimental device

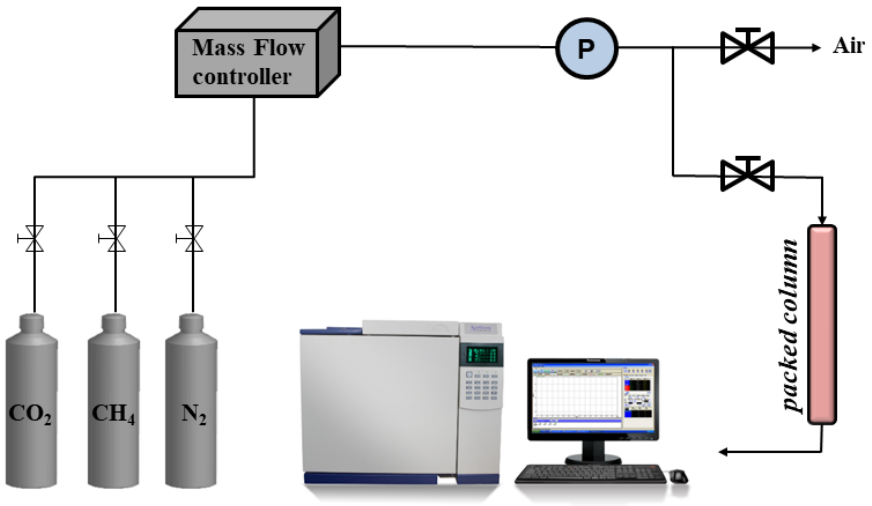

Figure. S1 Breakthrough experiments apparatus diagram.

4 Thermogravimetric curve

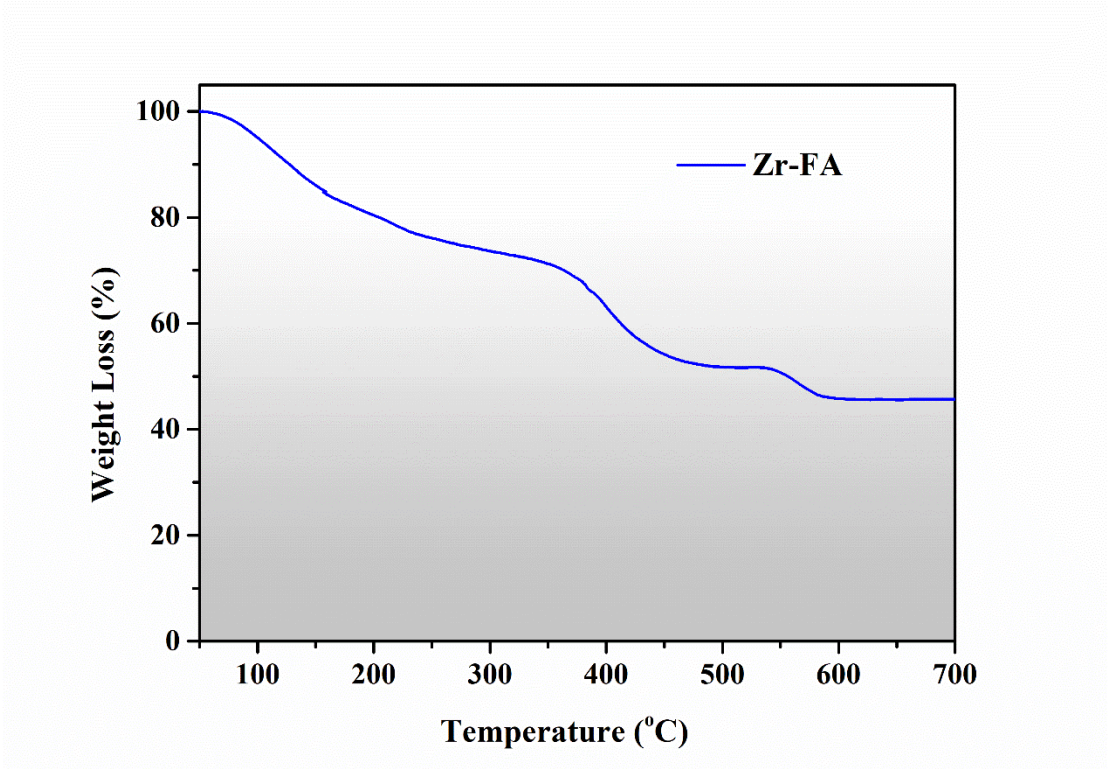

Figure. S2 The TGA curves of Zr-FA.

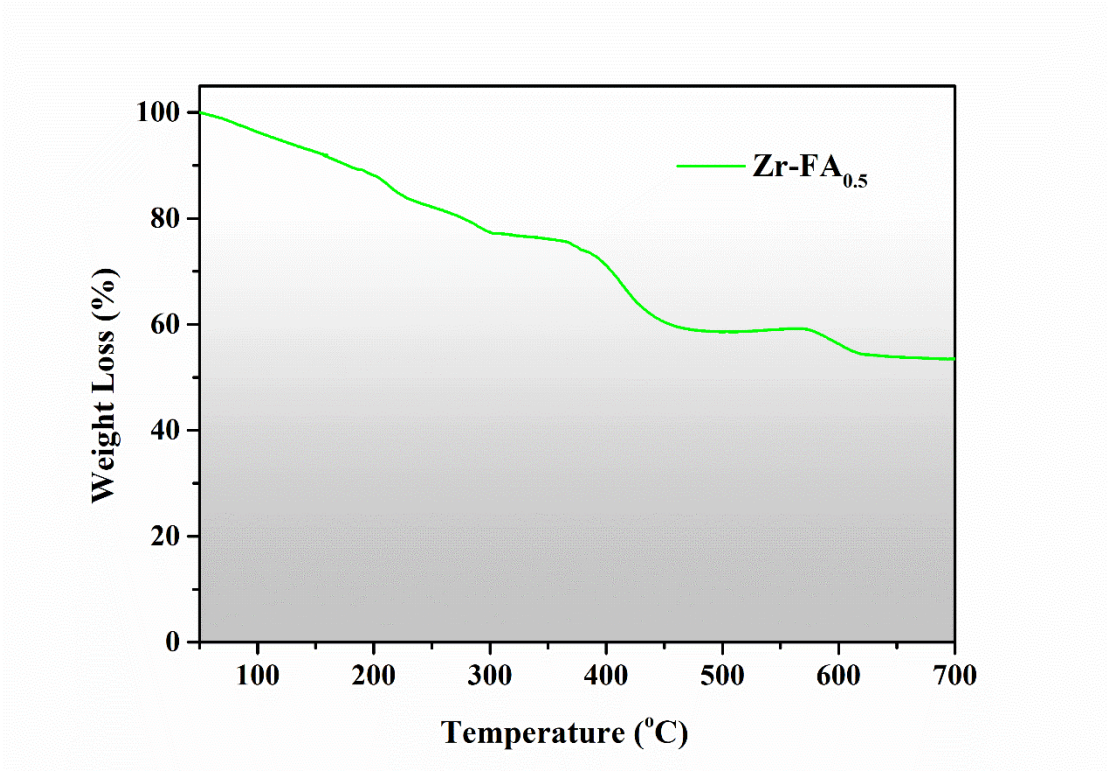

Figure. S3 The TGA curves of Zr-$FA_{0.5}$.

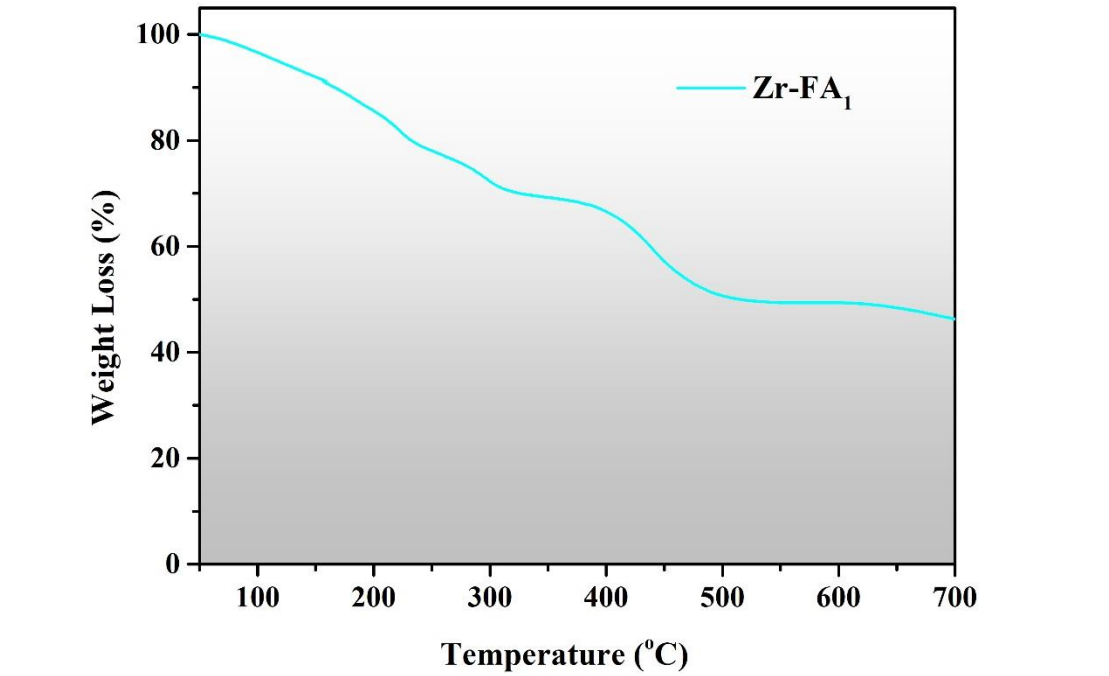

Figure. S4 The TGA curves of Zr-FA_1.

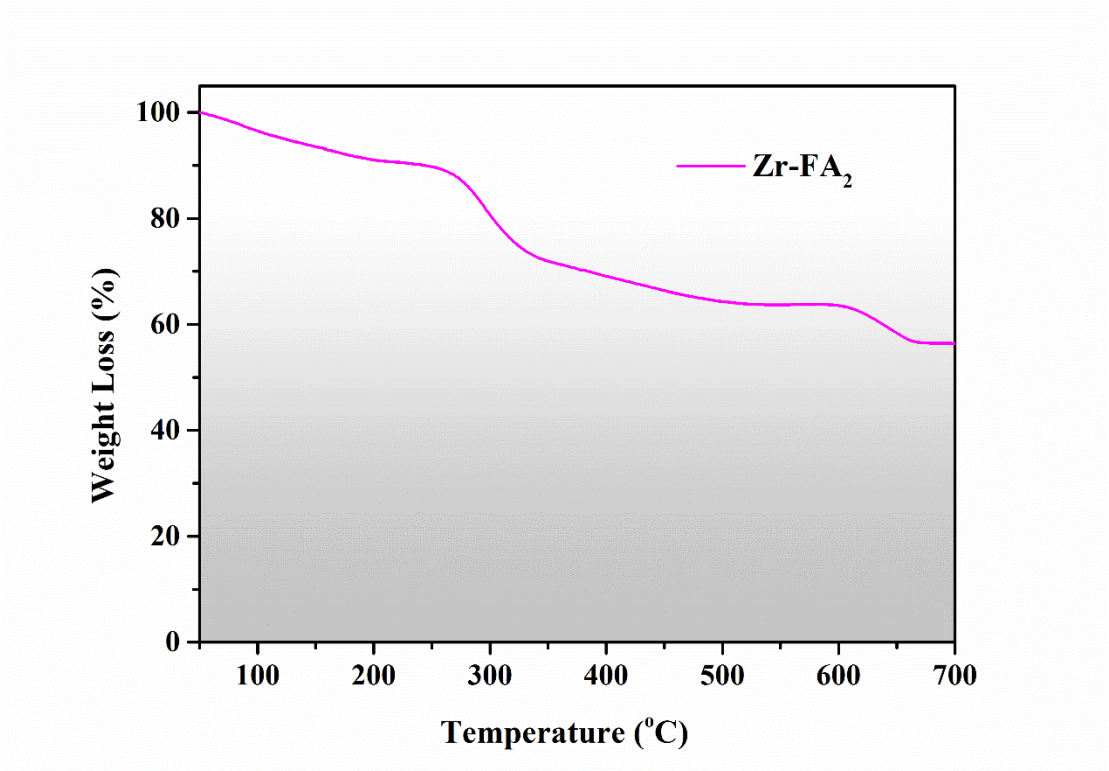

Figure. S5 The TGA curves of Zr-FA_2.

5 Gas adsorption and fitting curves

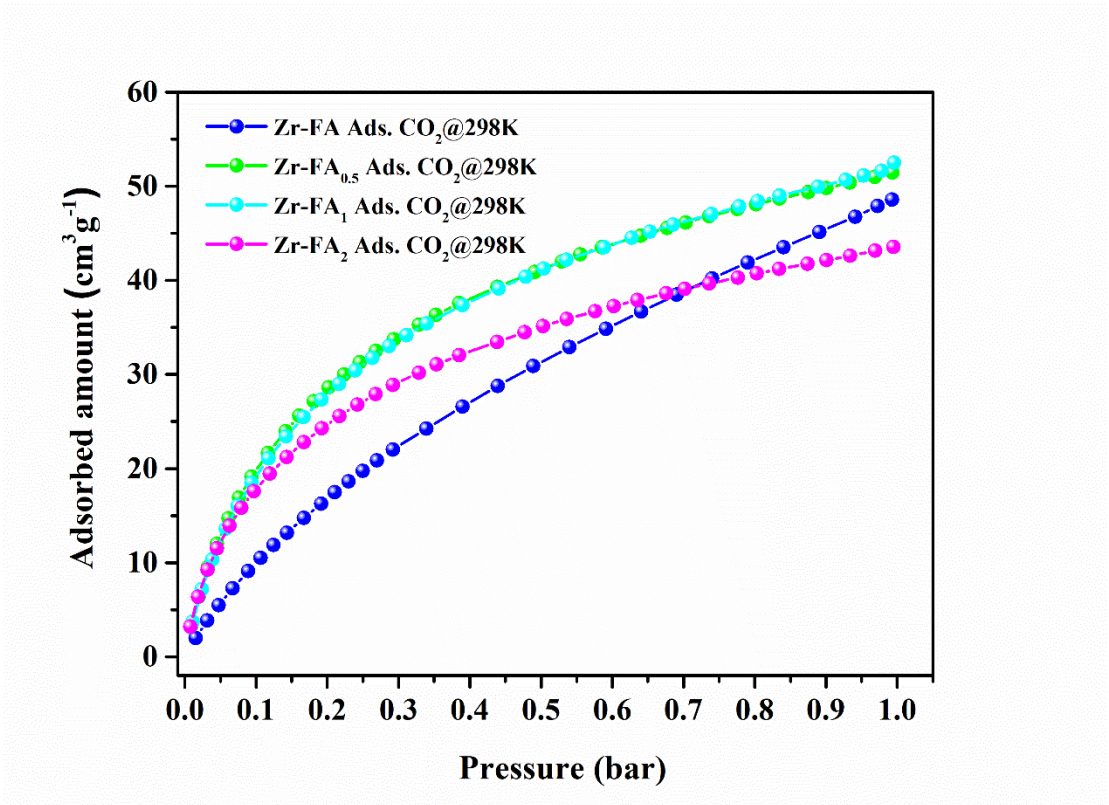

Figure. S6 Adsorption isotherms for CO_2 at 298 K on MOFs.

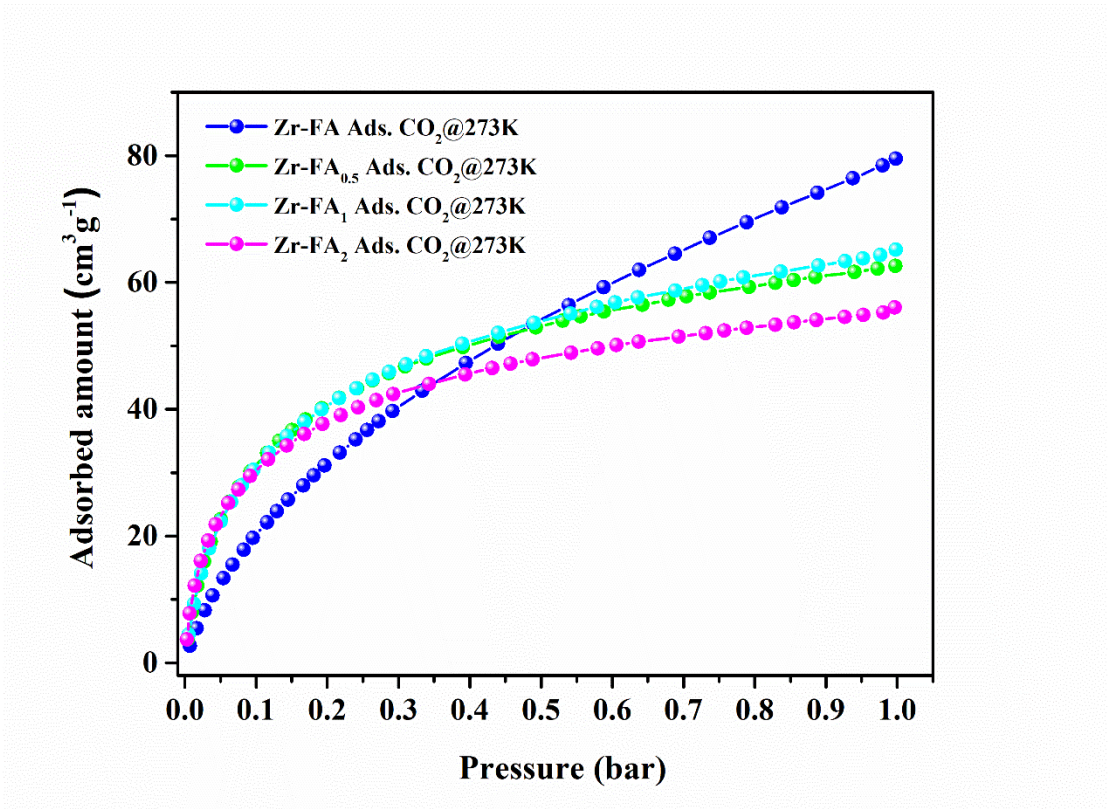

Figure. S7 Adsorption isotherms for CO_2 at 273 K on MOFs.

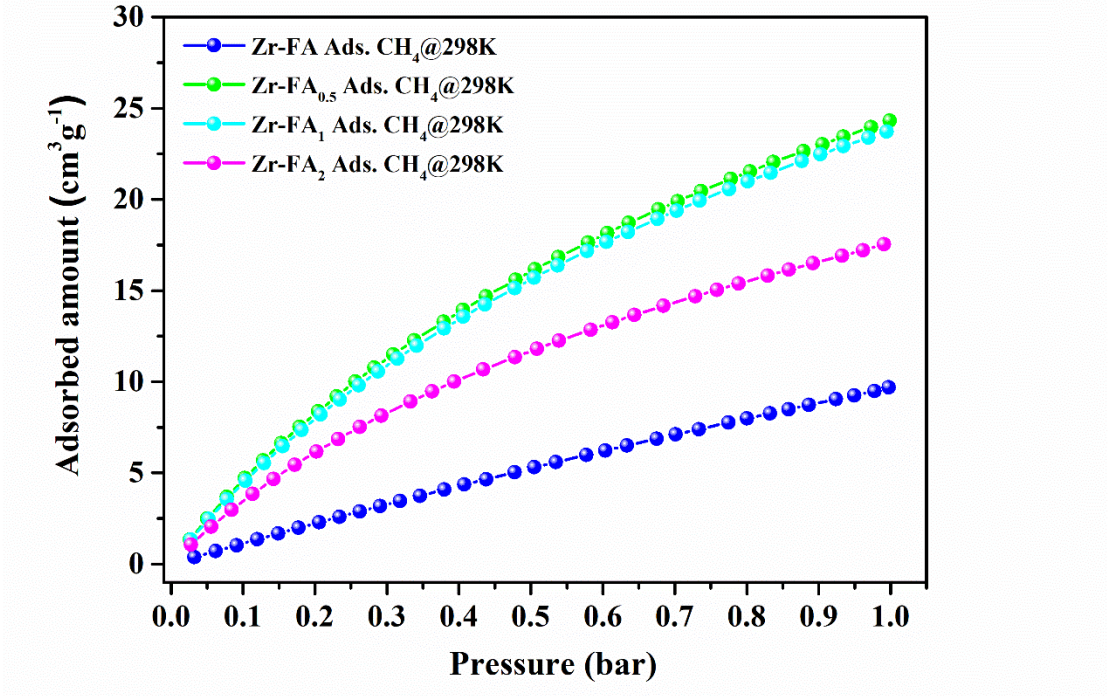

Figure. S8 Adsorption isotherms for CH_4 at 298 K on MOFs.

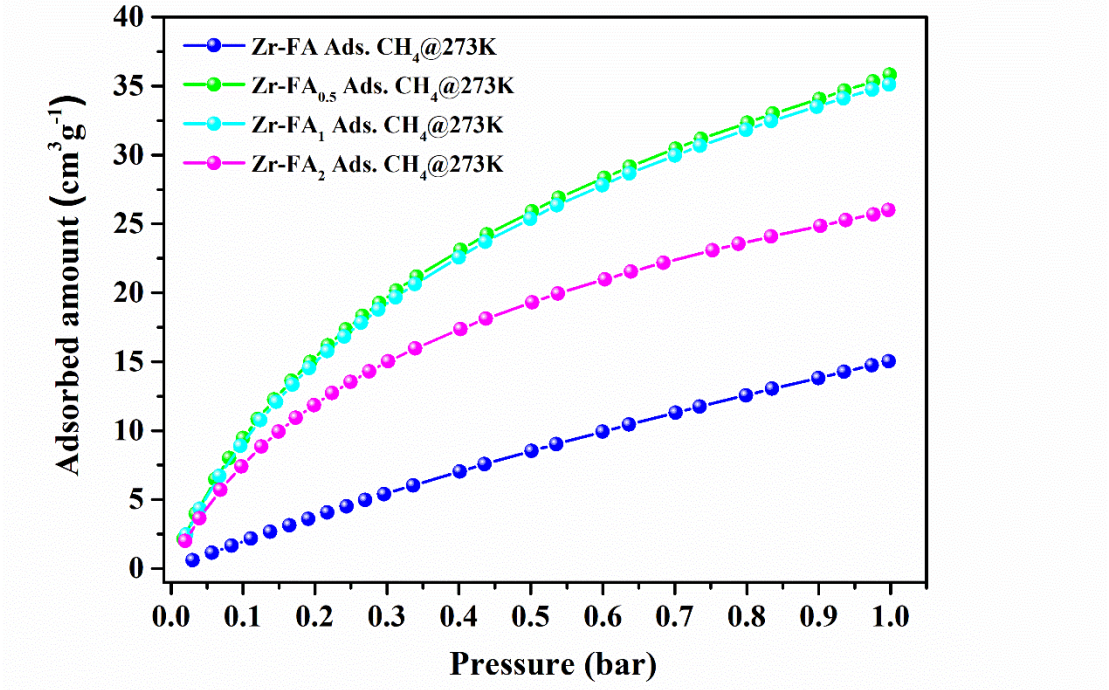

Figure. S9 Adsorption isotherms for CH_4 at 273 K on MOFs.

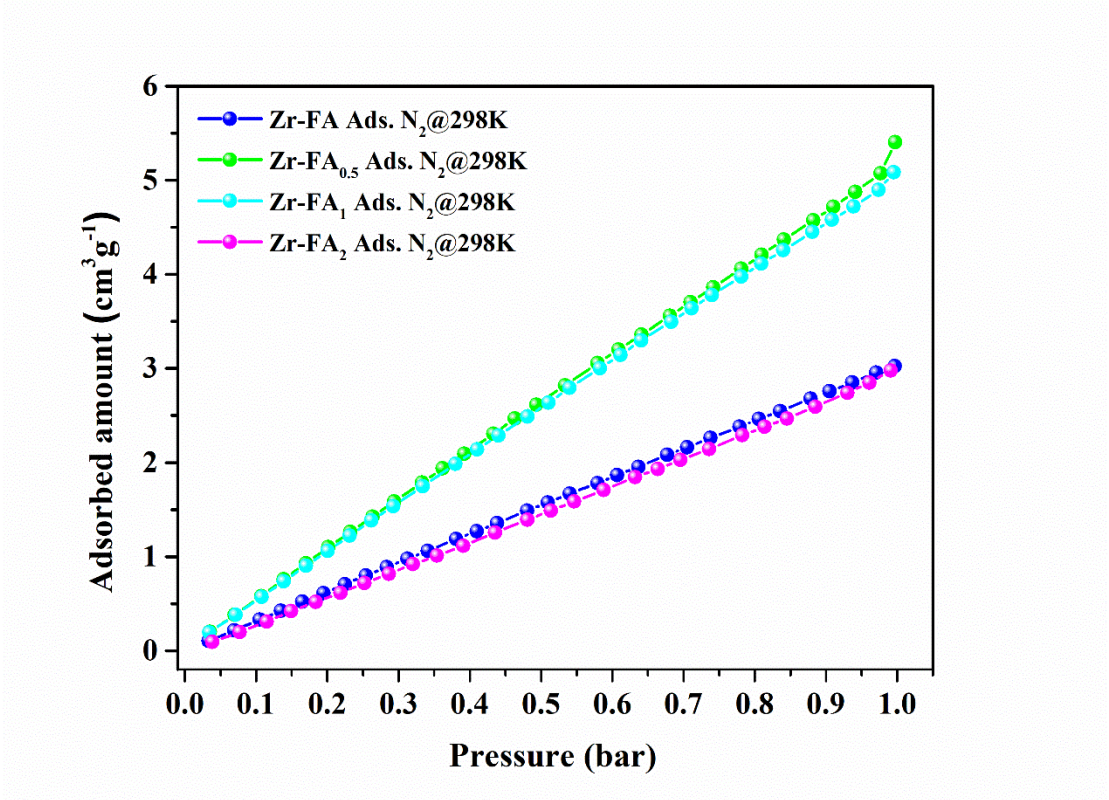

Figure. S10 Adsorption isotherms for N_2 at 298 K on MOFs.

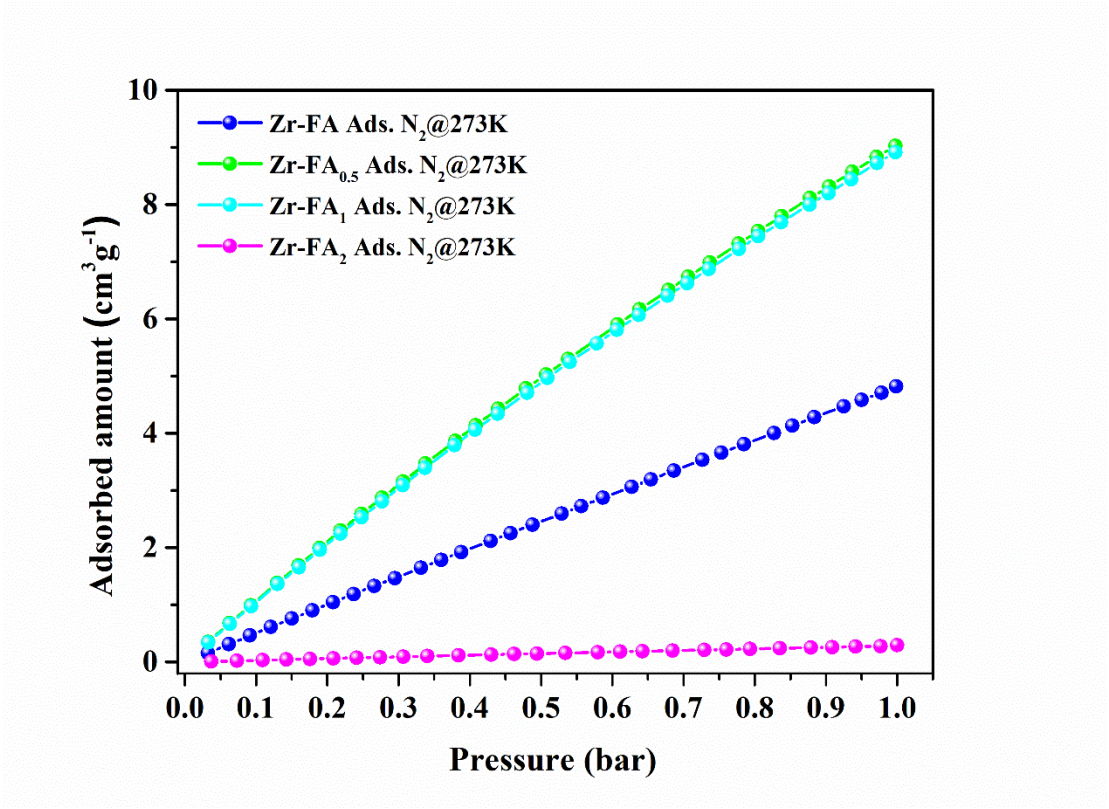

Figure. S11 Adsorption isotherms for N_2 at 273 K on MOFs.

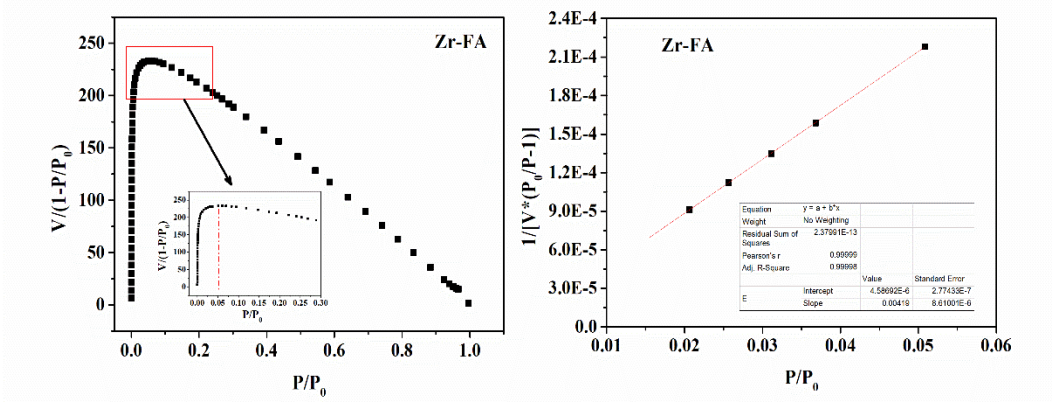

Figure. S12 The BET multipoint method to fit line for Zr-FA.

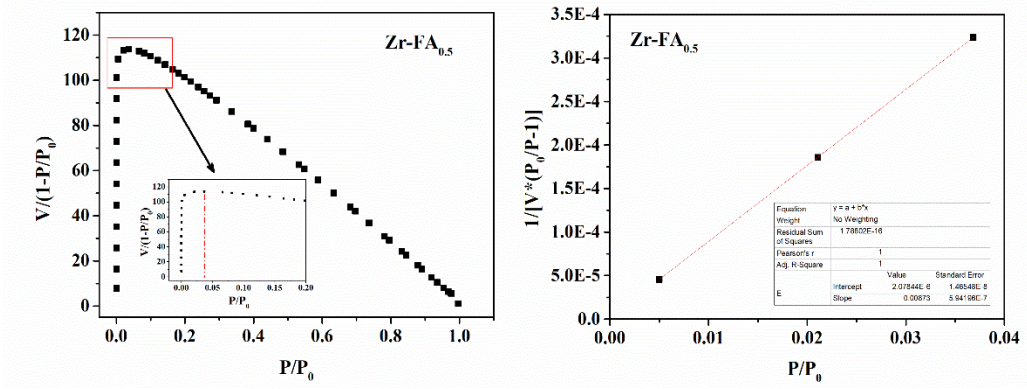

Figure. S13 The BET multipoint method to fit line for Zr-$FA_{0.5}$.

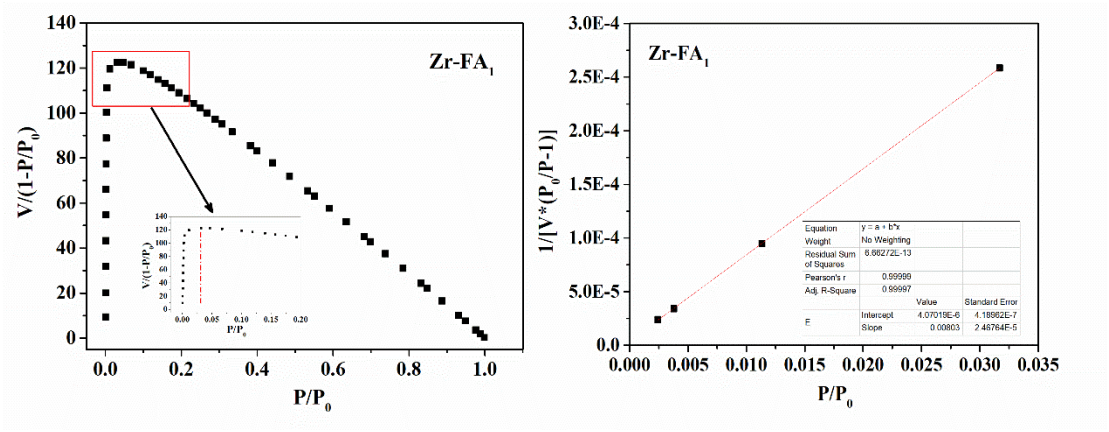

Figure. S14 The BET multipoint method to fit line for Zr-FA$_1$.

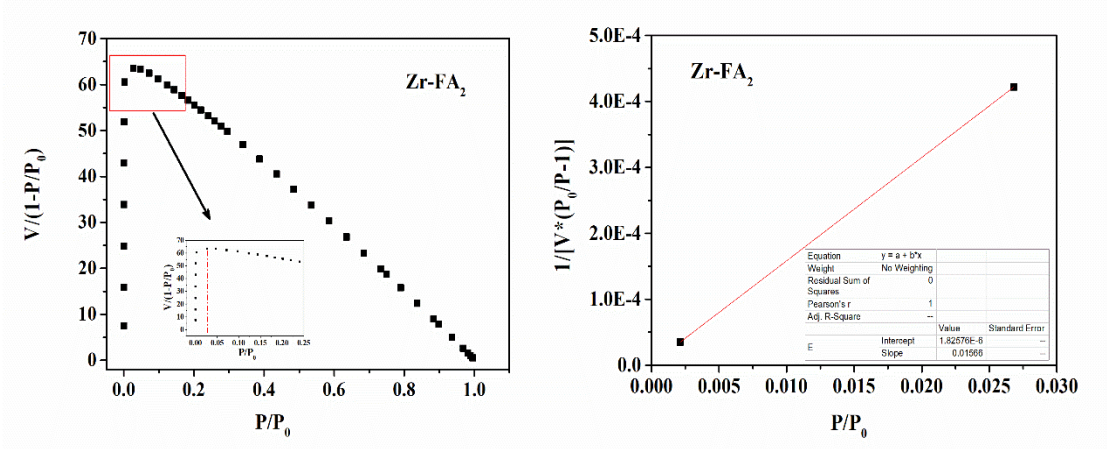

Figure. S15 The BET multipoint method to fit line for Zr-FA$_2$.

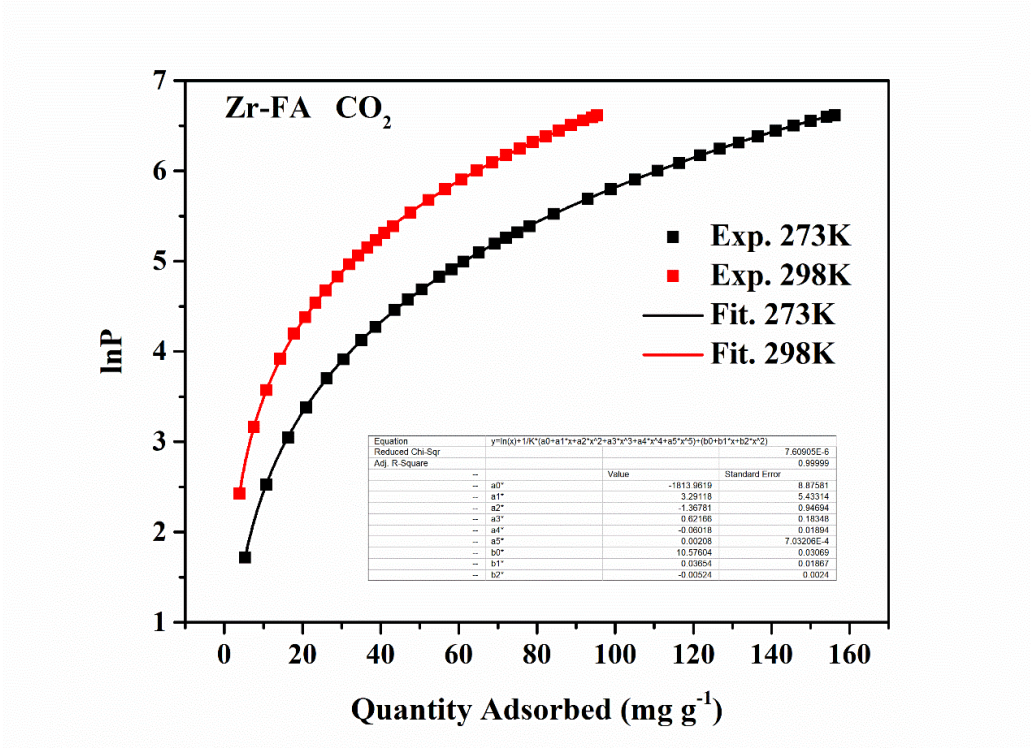

Figure. S16 The virial fitting of CO_2 sorption data for Zr-FA.

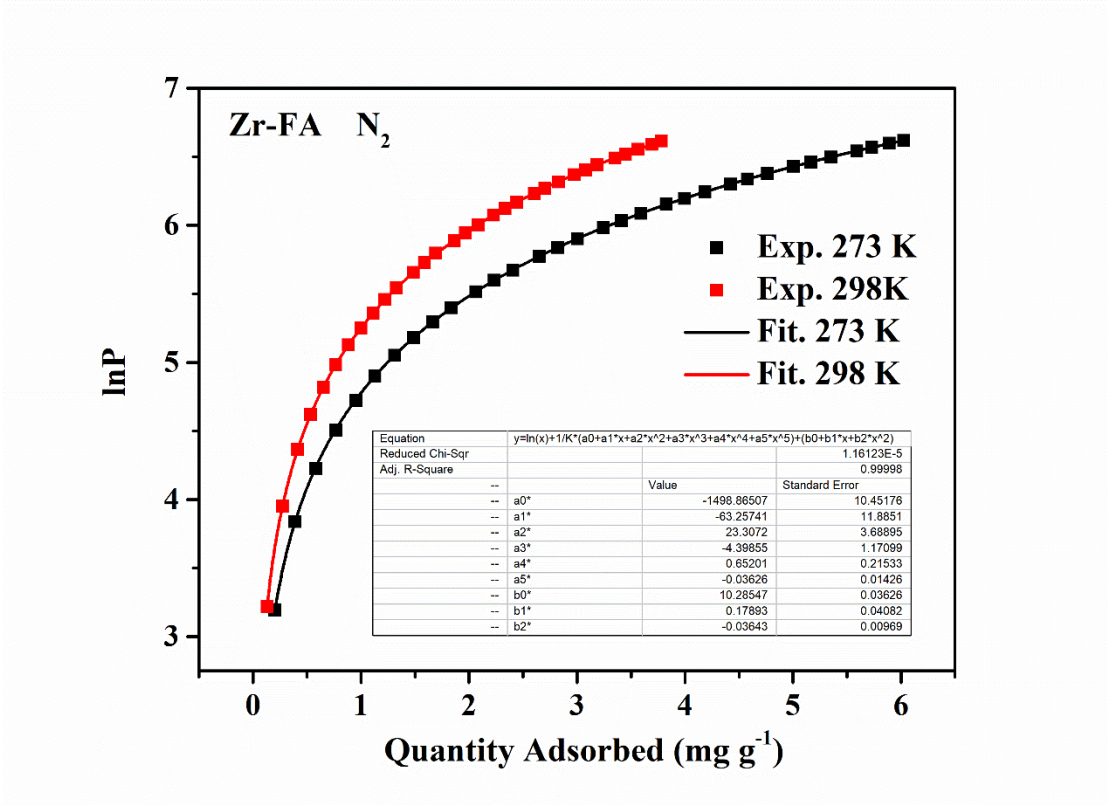

Equation	y=ln(x)+1/K*(a0+a1*x+a2*x^2+a3*x^3+a4*x^4+a5*x^5)+(b0+b1*x+b2*x^2)		
Reduced Chi-Sqr			1.16123E-5
Adj. R-Square			0.99998
--		Value	Standard Error
--	a0*	-1498.86507	10.45176
--	a1*	-63.25741	11.8851
--	a2*	23.3072	3.68895
--	a3*	-4.39855	1.17099
--	a4*	0.65201	0.21533
--	a5*	-0.03626	0.01426
--	b0*	10.28547	0.03626
--	b1*	0.17893	0.04082
--	b2*	-0.03643	0.00969

Figure. S17 The virial fitting of N_2 sorption data for Zr-FA.

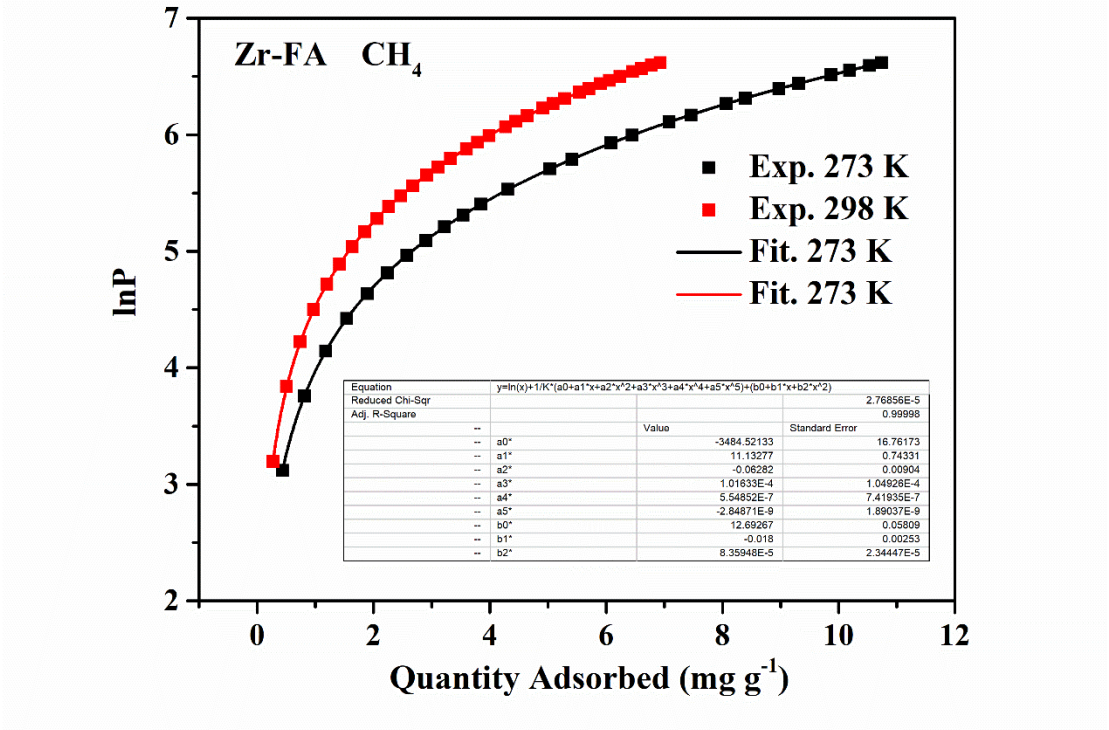

Equation	y=ln(x)+1/K*(a0+a1*x+a2*x^2+a3*x^3+a4*x^4+a5*x^5)+(b0+b1*x+b2*x^2)		
Reduced Chi-Sqr			2.76856E-5
Adj. R-Square			0.99998
--		Value	Standard Error
--	a0*	-3484.52133	16.76173
--	a1*	11.13277	0.74331
--	a2*	-0.06282	0.00904
--	a3*	1.01633E-4	1.04926E-4
--	a4*	5.54852E-7	7.41935E-7
--	a5*	-2.84871E-9	1.89037E-9
--	b0*	12.69267	0.05809
--	b1*	-0.018	0.00253
--	b2*	8.35948E-5	2.34447E-5

Figure. S18 The virial fitting of CH_4 sorption data for Zr-FA.

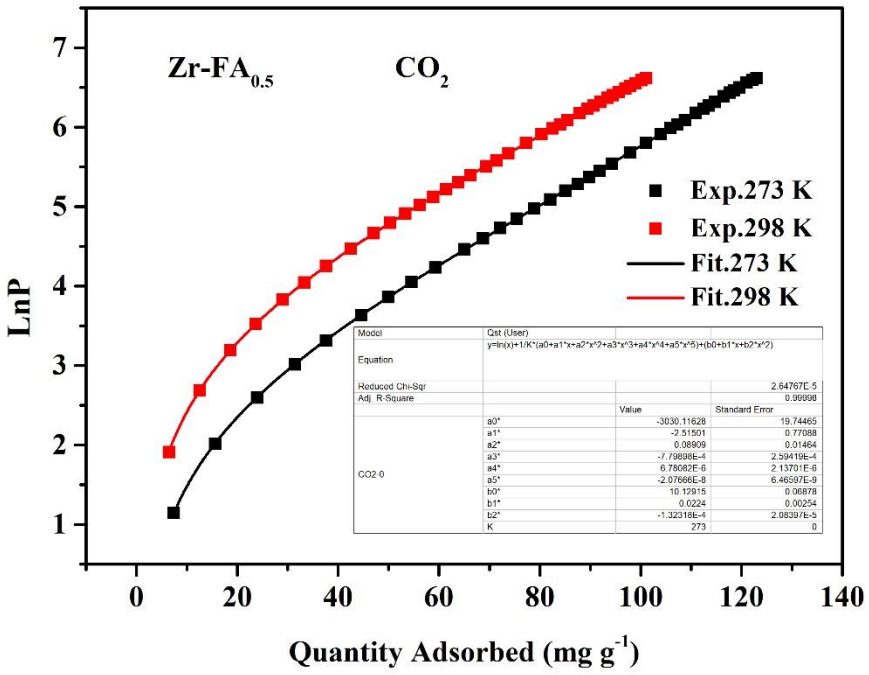

Figure. S19 The virial fitting of CO_2 sorption data for Zr-$FA_{0.5}$.

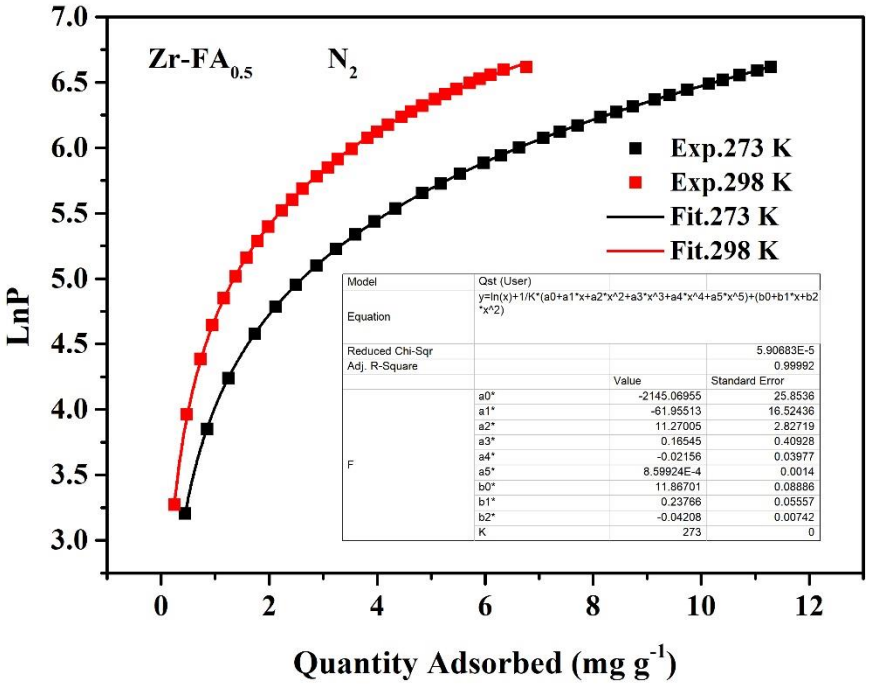

Figure. S20 The virial fitting of N_2 sorption data for Zr-$FA_{0.5}$.

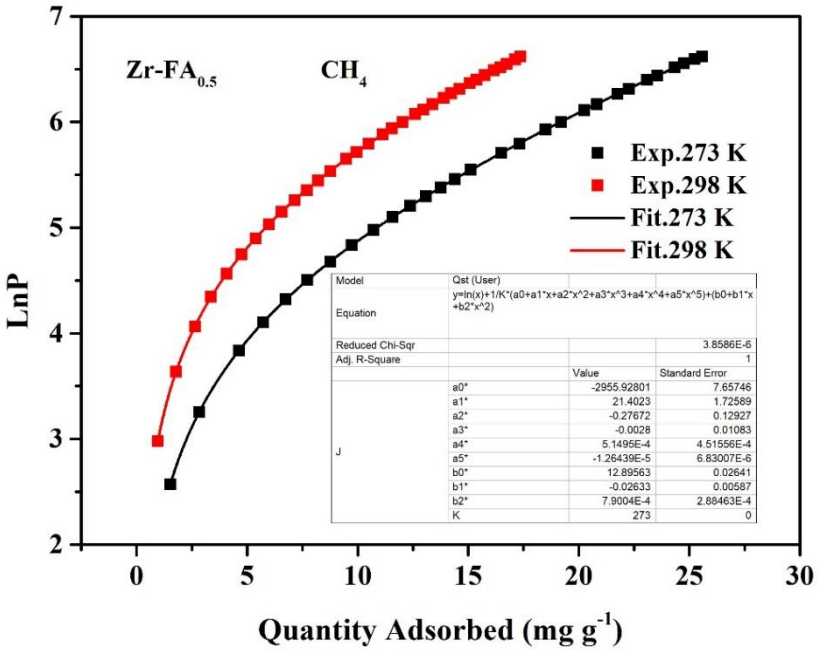

Figure. S21 The virial fitting of CH_4 sorption data for Zr-$FA_{0.5}$.

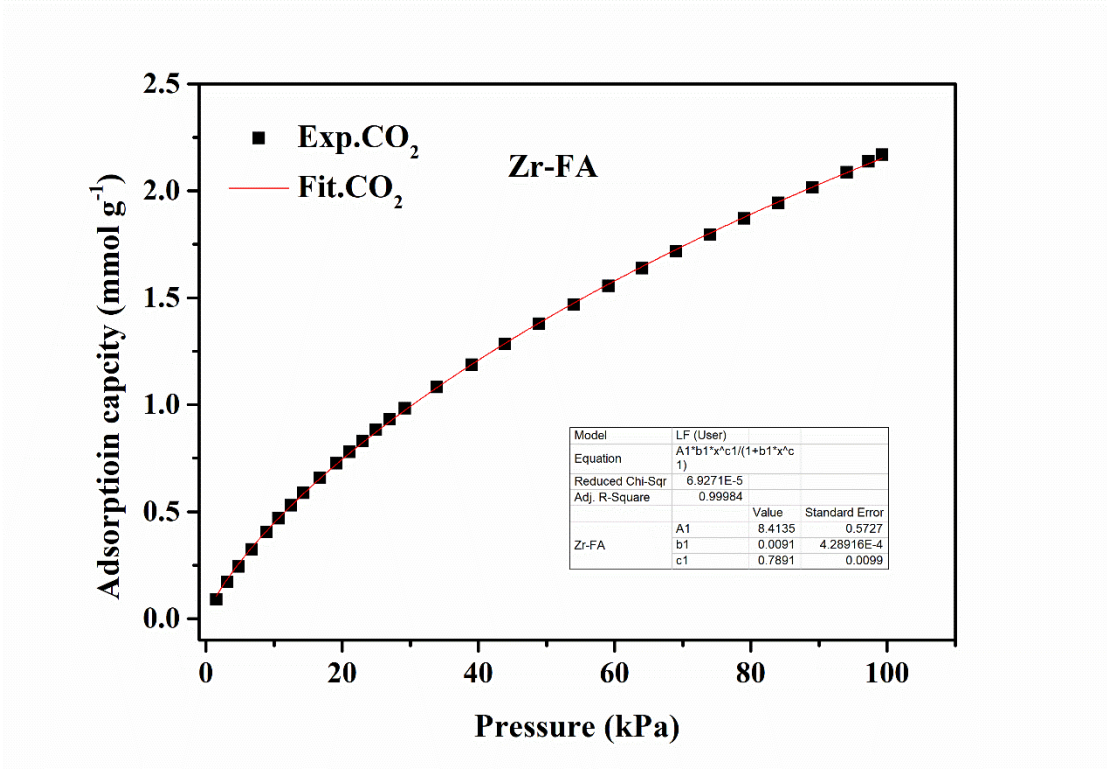

Figure. S22 CO_2 adsorption isotherms at 298 K in Zr-FA with Single-site Langmuir-Freundlich model fits.

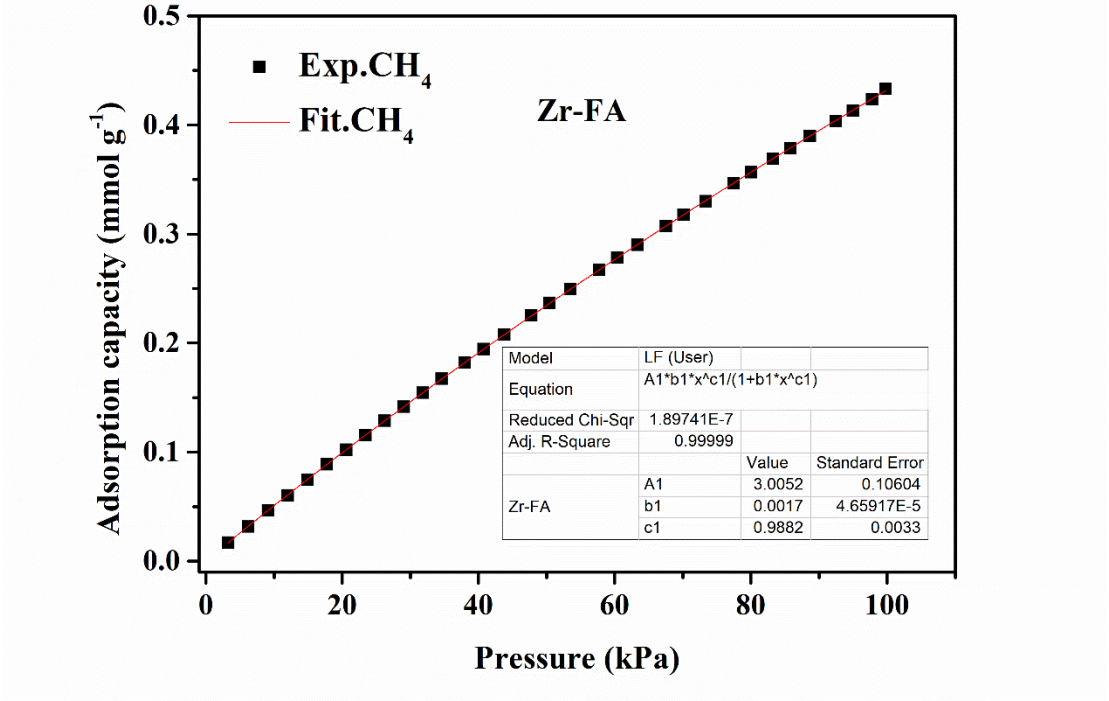

Figure. S23 CH_4 adsorption isotherms at 298 K in Zr-FA with Single-site Langmuir-Freundlich model fits.

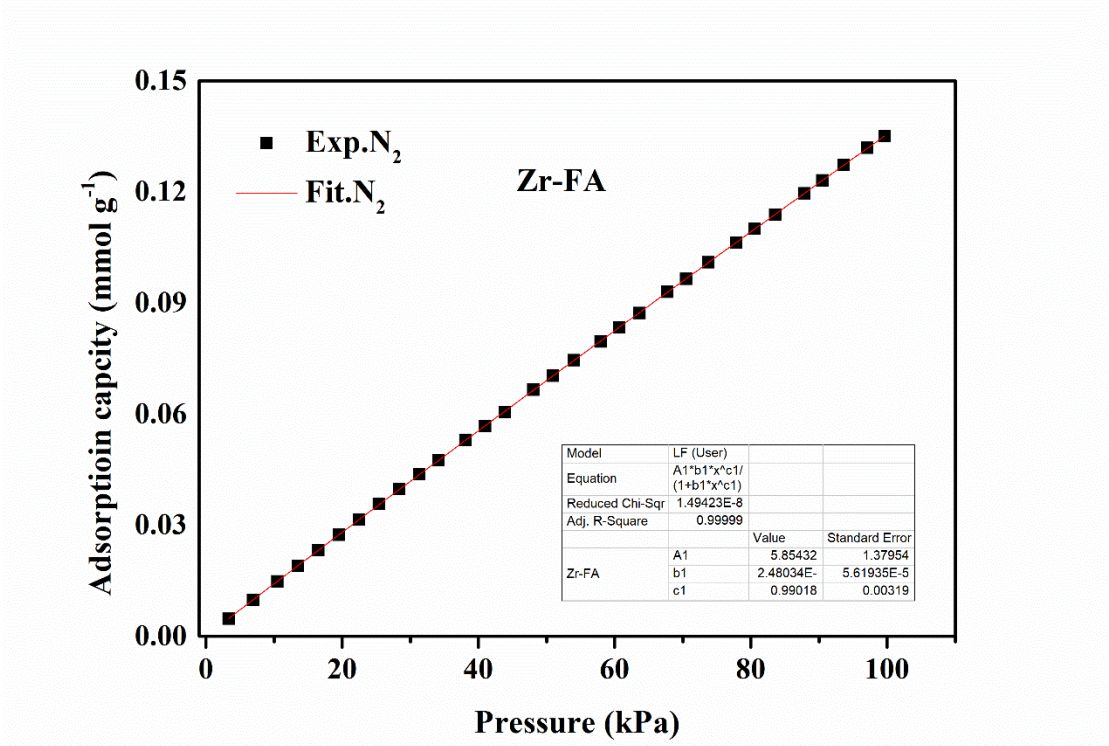

Figure. S24 N_2 adsorption isotherms at 298 K in Zr-FA with Single-site Langmuir-Freundlich model fits.

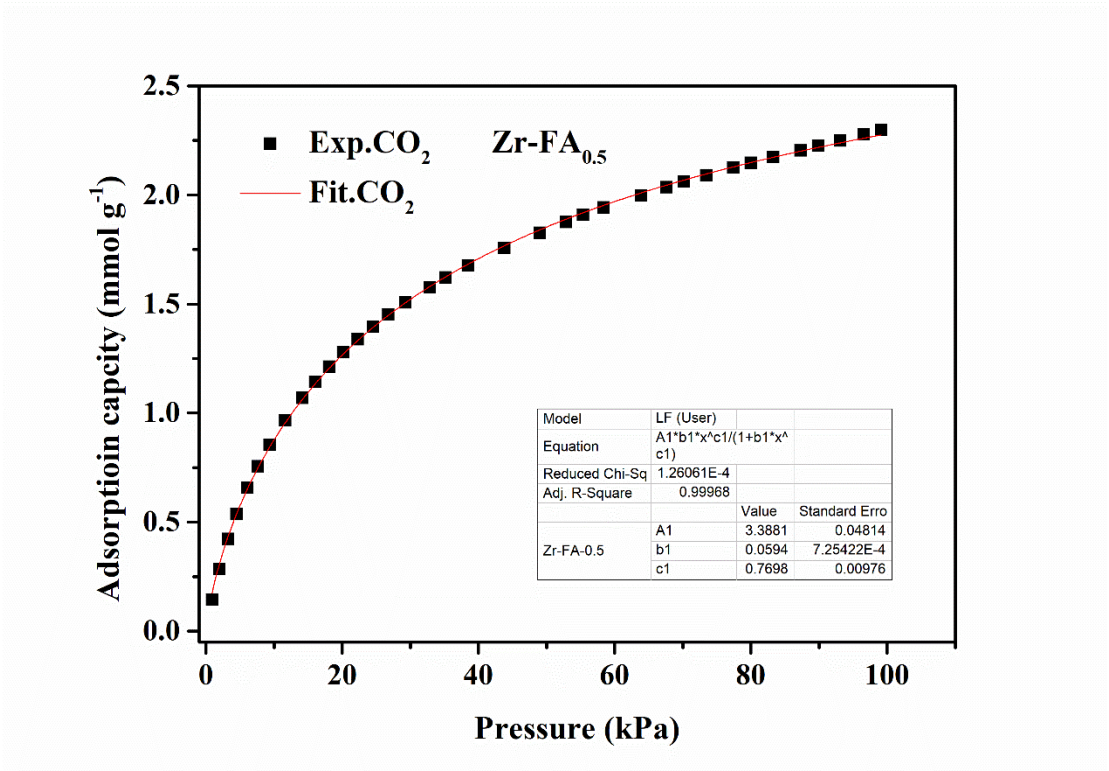

Figure. S25 CO_2 adsorption isotherms at 298 K in Zr-$FA_{0.5}$ with Single-site Langmuir-Freundlich model fits.

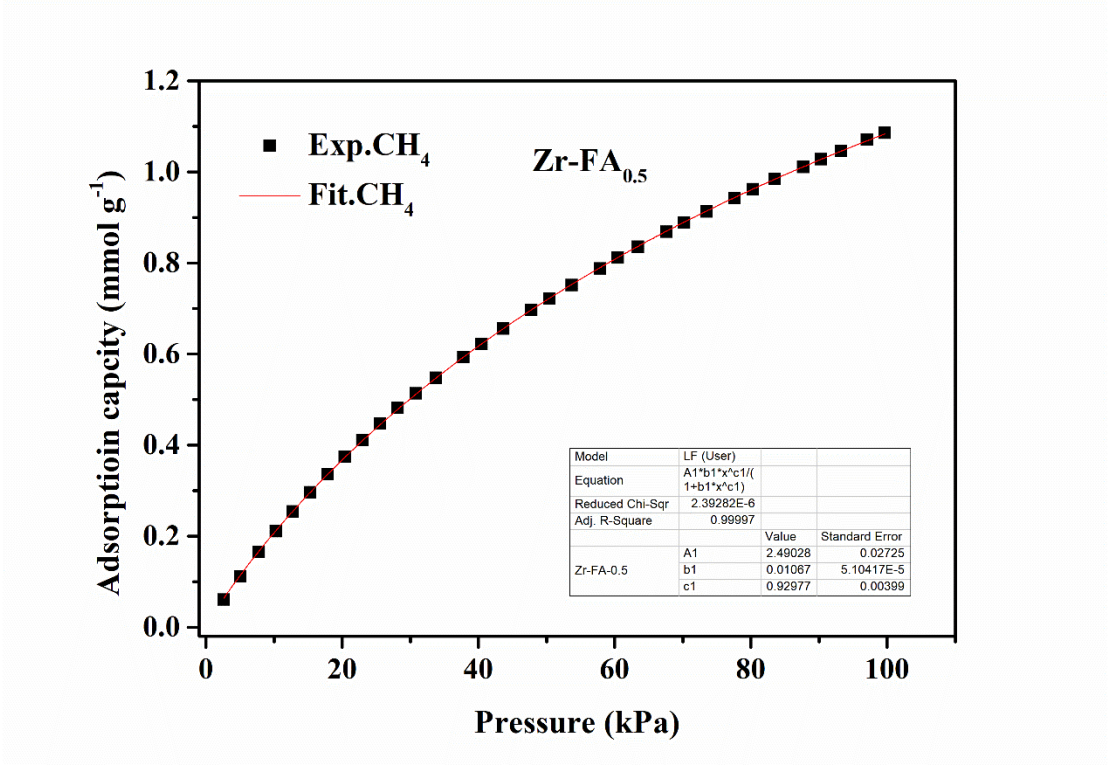

Figure. S26 CH_4 adsorption isotherms at 298 K in Zr-$FA_{0.5}$ with Single-site Langmuir-Freundlich model fits.

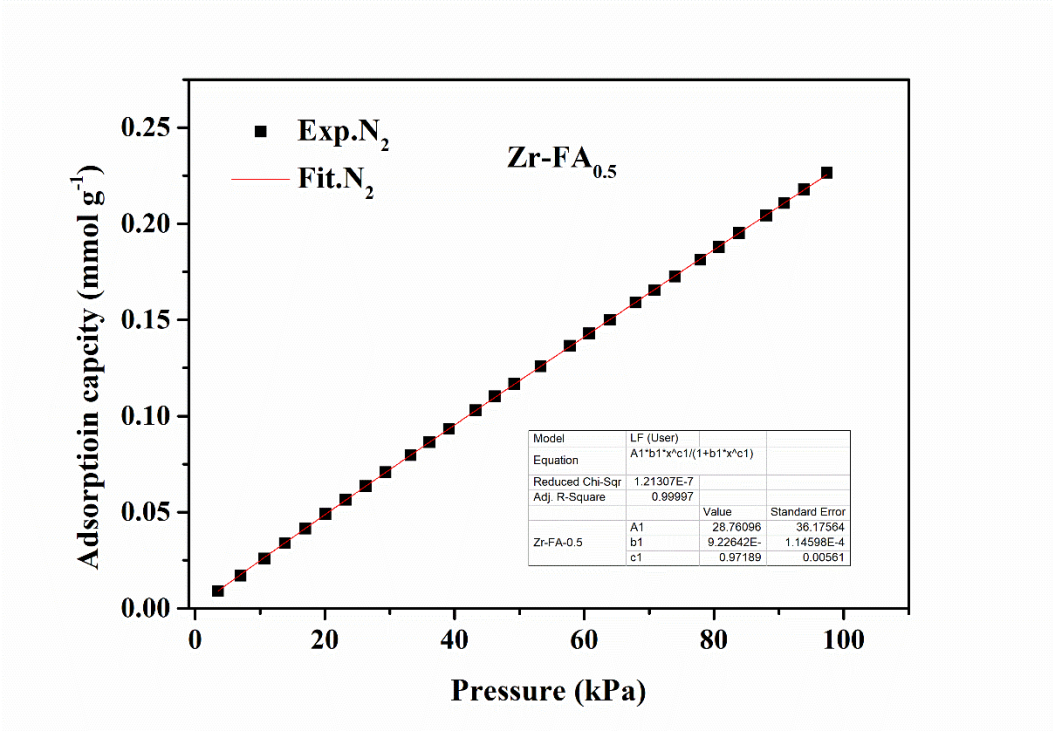

Figure. S27 N_2 adsorption isotherms at 298 K in Zr-$FA_{0.5}$ with Single-site Langmuir-Freundlich model fits.

Reference

1 D. A. Gómez-Gualdrón, P. Z. Moghadam, J. T. Hupp, O. K. Farha and R. Q. Snurr, *J. Am. Chem. Soc.*, 2016, **138**, 215–224.

2 K. A. G. Amankwab and J. A. Schwakz, *Carbon N. Y.*, 1995, **33**, 1313–1319.

3 I. Langmuir, *J. Am. Chem. Soc.*, 1918, **40**, 1361–1403.

4 J. W. Yoon, H. Chang, S. J. Lee, Y. K. Hwang, D. Y. Hong, S. K. Lee, J. S. Lee, S. Jang, T. U. Yoon, K. Kwac, Y. Jung, R. S. Pillai, F. Faucher, A. Vimont, M. Daturi, G. Férey, C. Serre, G. Maurin, Y. S. Bae and J. S. Chang, *Nat. Mater.*, 2017, **16**, 526–531.

5 R. Sips, *J. Chem. Phys.*, 1948, **16**, 490–495.

6 Y.A.B. Çengel and A. Michael, *McGraw-Hill*.

7 S. Dai, F. Nouar, S. Zhang, A. Tissot and C. Serre, *Angew. Chemie - Int. Ed.*, 2021, **60**, 4282–4288.